

Temporal and spatial Taylor's law: Application to Japanese subnational mortality rates

Yang Yang¹  | Han Lin Shang²  | Joel E. Cohen^{3,4,5} 

¹Department of Econometrics and Business Statistics, Monash University, Melbourne, Victoria, Australia

²Department of Actuarial Studies and Business Analytics, Macquarie University, Sydney, New South Wales, Australia

³Laboratory of Populations, The Rockefeller University, New York, New York, USA

⁴Earth Institute & Department of Statistics, Columbia University, New York, New York, USA

⁵Department of Statistics, University of Chicago, Chicago, Illinois, USA

Correspondence

Yang Yang, Department of Econometrics and Business Statistics, Monash University, Melbourne, VIC 3145, Australia.

Email: yang.yang3@monash.edu

Abstract

Taylor's law is a widely observed empirical pattern that relates the variances to the means of population densities. We present four extensions of the classical Taylor's law (TL): (1) a cubic extension of the linear TL describes the mean–variance relationship of human mortality at subnational levels well; (2) in a time series, long-run variance measures not only variance but also autocovariance, and it is a more suitable measure than variance alone to capture temporal/spatial correlation; (3) an extension of the classical equally weighted spatial variance takes account of synchrony and proximity; (4) robust linear regression estimators of TL parameters reduce vulnerability to outliers. Applying the proposed methods to age-specific Japanese subnational death rates from 1975 to 2018, we study temporal and spatial variations, compare different coefficient estimators, and interpret the implications. We apply a clustering algorithm to the estimated TL coefficients and find that cluster memberships are strongly related to prefectural gross domestic product. The time series of spatial TL coefficients has a decreasing trend that confirms the narrowing gap between rural and urban mortality in Japan.

KEYWORDS

long-run variance, loss function, spatial dependence, Taylor's power law of fluctuation scaling, temporal dependence

This is an open access article under the terms of the [Creative Commons Attribution-NonCommercial-NoDerivs License](https://creativecommons.org/licenses/by-nc-nd/4.0/), which permits use and distribution in any medium, provided the original work is properly cited, the use is non-commercial and no modifications or adaptations are made.

© 2022 The Authors. *Journal of the Royal Statistical Society: Series A (Statistics in Society)* published by John Wiley & Sons Ltd on behalf of Royal Statistical Society.

1 | INTRODUCTION

Demographers often study changes in the human population density, which is the number of people per unit of area, of different regions in terms of the births and deaths within each region and migration among regions through a multistate modelling framework (e.g. Rogers, 1995, 2008). Ecologists also share this multistate modelling framework for studying the density of spatially separated populations of a single or of multiple species (e.g. Cohen & Saitoh, 2016; Cohen et al., 2013, 2016; Dey & Joshi, 2006; Gilpin & Hanski, 1991; Hanski, 1999). In entomology, Taylor (1961) and his collaborators (Perry & Taylor, 1985; Taylor, 1984; Taylor & Woiwod, 1980, 1982; Taylor et al., 1978, 1980) observe that in many species, the logarithm of the variance of the density of a set of comparable populations is an approximately linear function of the logarithm of the mean density, for example $\log(\text{variance}) = \log(a) + b \times \log(\text{mean})$ for some parameters $a > 0$ and b . Throughout this paper, we consider the logarithm to base 10. This relationship became known as Taylor's law (TL) of fluctuation scaling (Eisler et al., 2008; Taylor, 2019).

Mortality rates as a statistical summary of a population's survival patterns affect population growth and density (e.g. Tarsi & Tuff, 2012). Japan, as the nation with the highest life expectancies at age 65 and above among all countries in the world, is facing tremendous pressure on its existing pension, health and aged care systems caused by population ageing (Coulmas, 2007). Identifying the spatial variation of Japanese mortality across all 47 prefectures and temporal trends of mortality could assist government policymakers and planners in developing national pension reforms.

There are three main methodological contributions in this paper. Applications of TL to human age-specific mortality rates have described linear relationships of log variance to log mean for national populations of a dozen OECD countries including Japan (see, e.g. Bohk et al., 2015; Cohen et al., 2018a,b). Recently, a quadratic extension of TL is considered in modelling US county population distributions by Xu and Cohen (2019). TL has also been used to study human population by Xu et al. (2017) and Cohen et al. (2018) and Naccarato and Benassi (2018). The TL coefficients can be seen as a summary statistic for analysing human mortality. One can apply a clustering algorithm, such as *K*-means, based on the estimated TL coefficients to identify cluster memberships. Analysing differentials in mortality of various prefectures is beneficial for determining the national and subnational administrations' allocation of current and future resources. We further extend TL to include a cubic term and show that the proposed model can better capture the mean-variance relationship of subnational age-specific mortality rates in Japan. The second contribution of this paper is that we compute the long-run variance instead of variance alone. In time series analysis, long-run variance captures not only the variance but also includes autocovariance. Thus, the long-run variance encompasses more information and is a more suitable summary statistic for a time series. By regressing the logarithm of the long-run variance against the logarithm of the mean, we obtain modified TL coefficient estimators. To sum up temporal and spatial variations of mortality rates in a single parameter, we also consider a novel spatial-temporal TL based on a long-run spatial variance measure. Third, in using TL to describe Japanese age-specific mortality, short-term fluctuations of mortality caused by natural disasters, such as earthquakes and tsunamis, should be excluded from the computation of the long-term TL coefficients (Aida et al., 2017). To address this issue, we consider a robust estimator to down-weight the influence of unusual mortality observations. In particular, we adopt the Hampel function (Hampel, 1974) and Tukey's biweight function (see, e.g. Hoaglin et al., 1983) in estimating the parameters of our extended TL for Japanese subnational age-specific mortality rates from 1975 to 2018, and

compare the robust estimates to the ordinary least squares (OLS) estimates of Bohk et al. (2015) and Cohen et al. (2018a).

Throughout this paper, we consider three variations of TL models: the spatial TL, the temporal TL and the spatial–temporal TL. First, for each of the 47 prefectures of Japan, we regress the logarithm of variance of age-specific mortality rates to the logarithm of the mean for years from 1975 to 2018. This approach estimates a temporal TL. Second, for each year during the considered 44-year period, a regression model is fitted to the logarithm of mean and the logarithm of variance of age-specific mortality rates of various geographical locations. This approach estimates a spatial TL. The current paper is the first to apply spatial or temporal TL to study subnational mortality patterns to the best of our knowledge. Third, we propose and apply a version of TL where the dependent variable is an integrated measure of both temporal and spatial variation, taking account of both temporal and spatial correlations.

The rest of the paper is organized as follows: In Section 2, we introduce the Japanese subnational mortality data before presenting the classical and robust estimators for estimating the slope parameters in the spatial or temporal TL. In Section 3, we present extensions of TL estimation methods. In Section 4, we compare performances of different TL estimation methods using the weighted spatial TL, long-run temporal TL and spatial–temporal TL to analyse the Japanese mortality data. In Section 5, we summarize our main empirical discoveries about Japan’s mortality patterns by prefecture and present some ideas on how the methodology presented can be further extended.

2 | DATA AND METHODS

2.1 | Age-specific mortality rates for 47 Japanese prefectures

Many OECD countries consider the remarkable increase in life expectancy as one of the greatest achievements of the last century (OECD, 2019). As population ageing has been one of the main driving forces in pension policies and reforms, the patterns of improvement in age-specific mortality rates have attracted the interests of government policymakers and planners. In particular, subnational forecasts of age-specific mortality rates help inform policy within local regions.

We study Japanese age-specific mortality rates disaggregated by sex group (male, female and total) and by 47 prefectures from 1975 to 2018 obtained from the Japanese Mortality Database (2021). Ages from 0 to 99 are considered in single years of completed age, while the last age group contains all ages at and beyond 100, leading to a total of 101 (e.g. 0, 1, ..., 100) integer ages. Denote the death counts at age u in year t as $d_t(u)$ and the population of age u at 30 June in year t (also known as the ‘exposure-to-risk’ or as ‘life-years lived’) as $L_t(u)$. We consider continuous functions of mortality such that

$$\mathcal{Y}_t(u) = \frac{d_t(u)}{L_t(u)}, \quad u \in [0, 100], \quad t = 1975, \dots, 2018.$$

Figure 1 shows rainbow plots of the observed female and male age-specific mortality curves in Japan from 1975 to 2018 in \log_{10} scale. The time ordering of the curves follows the colour order of a rainbow, where curves from the distant past are shown in red and the more recent curves are shown in purple. The figures show typical mortality curves for a developed country. The pattern

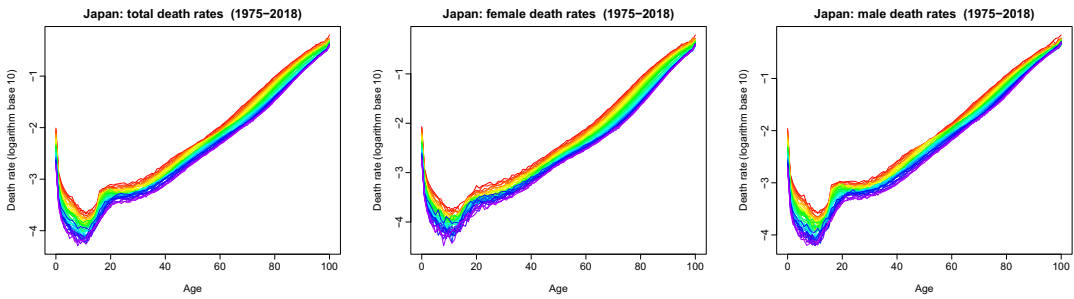


FIGURE 1 Japanese age-specific mortality rates of females, males and totals (both sexes combined) from age 0 to 100+ annually from 1975 to 2018, on \log_{10} scale. The curves from the distant past are shown in red, while the more recent curves are shown in purple. [Colour figure can be viewed at [wileyonlinelibrary.com](https://onlinelibrary.wiley.com/doi/10.1111/rssc.12899)]

begins with rapidly decreasing mortality rates in the early years of life, followed by an increase during the teenage years, a mortality bump (greater for males than females) for young adults and a steady, roughly exponential rise from about the age of 30. Females have lower mortality rates than males for all ages.

2.2 | Comparison of prefectures with national averages

Figure 2 depicts the logarithm of the ratio of each age-specific mortality rate for each prefecture to the average age-specific mortality rates for the whole country, allowing relative mortality comparisons to be made. Blue represents positive values, and orange denotes negative values. The prefectures are ordered geographically from north to south. The most northerly prefecture (Hokkaido) is at the top of the panels, and the most southerly prefecture (Okinawa) is at the bottom.

The top row of panels shows mortality rates for each prefecture and age, averaged over all years. There are great differences between the prefectures for children, especially females, possibly due to socio-economic differences and accessibility of health services. The most southerly prefecture, Okinawa, has particularly low mortality rates for older people; this is consistent with the extreme longevity for which Okinawa is famous (see, e.g. Suzuki et al., 2004; Takata et al., 1987; Willcox et al., 2007).

The bottom row of panels shows mortality rates for each prefecture and year, averaged over all ages. Three observations with unusually high mortality rates are highlighted with dark blue. In 2011, in prefectures Miyagi (4) and Iwate (3), there was a large increase in mortality compared to other prefectures. These are northern coastal regions, and the excessive relative mortality is due to the tsunami of 11 March 2011. There is a corresponding decrease in relative mortality in some other prefectures. In 1995, an increase in mortality for prefecture Hyōgo (28) corresponds with the Kobe (great Hanshin) earthquake of 17 January 1995.

2.3 | Classical estimation of the slope parameter

Taylor (1961), following several proposals by earlier ecologists, popularized a power law to describe a pattern in ecology regarding the spatial or temporal variability of population density.

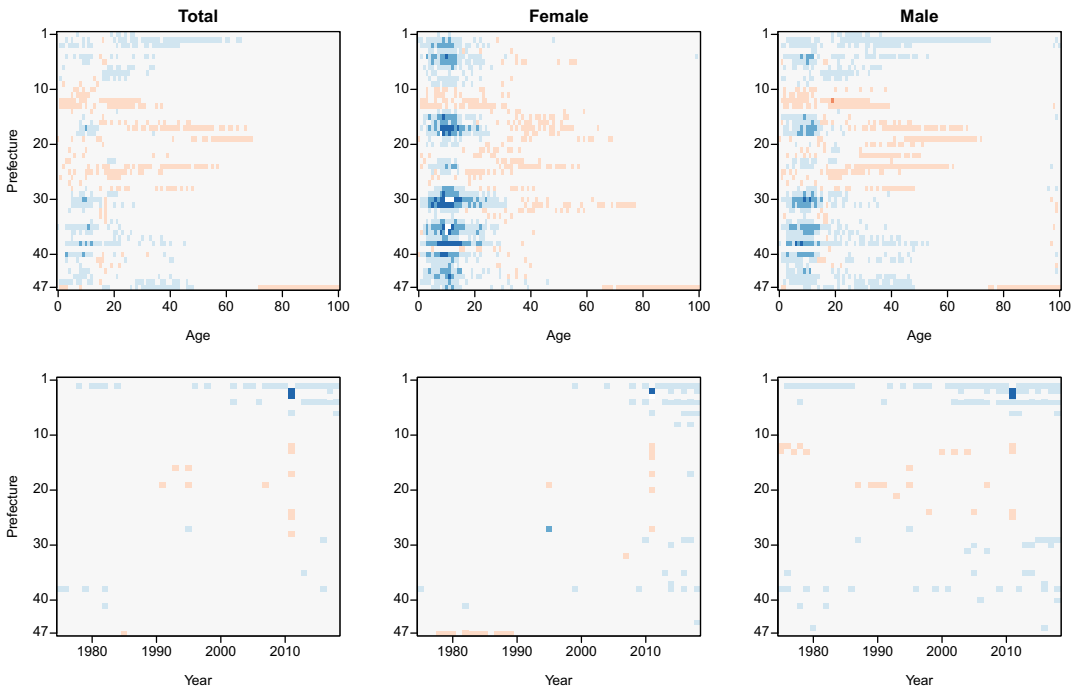


FIGURE 2 Mortality rates above the national average in blue and below the national average in orange, for each prefecture and age (top three panels) and each prefecture and year (bottom three panels). The top panel shows mortality rates averaged over the years, while the bottom panel shows those averaged over the ages. Prefectures are numbered geographically from north (Hokkaido, 1) to south (Okinawa, 47). [Colour figure can be viewed at [wileyonlinelibrary.com](https://onlinelibrary.wiley.com/doi/10.1111/rssa.12859)]

Taylor’s law (TL) describes a linear relationship between the logarithms of the variance of nonnegative measurements P (e.g. population size, density or mortality rates) and the associated mean

$$\log[\text{Var}(P)] = \log a + b \cdot \log[E(P)] + \epsilon, \tag{1}$$

where $a > 0$ and b are both constants, and ϵ is the Gaussian error with mean zero and constant variance. Equation (1) is a simple linear model. Unlike the intercept, which depends on the unit of measurement, the slope parameter is independent of the measurement unit. As the logarithm of $E(P)$ increases by one, the logarithm of $\text{Var}(P)$ increases by a constant b . The parameters a and b are usually estimated by OLS.

Temporal and spatial TL require different definitions of $\text{Var}[\mathcal{Y}_t(u)]$ and $E[\mathcal{Y}_t(u)]$. Let $N = 47$ be the number of prefectures, and let $T = 44$ be the number of observation periods. A particular series u in prefecture j has temporal mean and temporal variance defined as

$$\begin{aligned} E_{\text{Temporal}}[\mathcal{Y}^j(u)] &= \frac{1}{T} \sum_{t=1}^T \mathcal{Y}_t^j(u), \quad j = 1, \dots, N, \\ \text{Var}_{\text{Temporal}}[\mathcal{Y}^j(u)] &= \frac{1}{T-1} \sum_{t=1}^T \left[\mathcal{Y}_t^j(u) - E_{\text{Temporal}}[\mathcal{Y}^j(u)] \right]^2. \end{aligned} \tag{2}$$

In contrast, a particular series u in year t has spatial mean and spatial variance defined as

$$\begin{aligned} E_{\text{Spatial}}[\mathcal{Y}_t(u)] &= \frac{1}{N} \sum_{j=1}^N \mathcal{Y}_t^j(u), \quad t = 1, \dots, T, \\ \text{Var}_{\text{Spatial}}[\mathcal{Y}_t(u)] &= \frac{1}{N-1} \sum_{j=1}^N \left[\mathcal{Y}_t^j(u) - E_{\text{Spatial}}[\mathcal{Y}_t(u)] \right]^2. \end{aligned} \quad (3)$$

The expression (3) weights each prefecture equally. By contrast, Cohen et al. (2013) evaluated a spatial TL for the populations of Norwegian regions, counties and municipalities weighting each administrative unit equally, or by its population, or by its land area. These other weighting possibilities may be worth exploring in the future. Benassi and Naccarato (2019) considered weighting spatial population density in Italy according to surface of each area and population density in each area.

2.4 | Outliers for linear TL models

Apart from years that witnessed high mortality due to natural disasters, as shown in the bottom panel in Figure 2, there are ages at which observed mortality rates deviate from TL during the considered time period. Before applying the classical temporal and spatial TL specifications introduced in Section 2.3 to Japanese subnational age-specific mortality rates, we first identify observations that distort the linear mean–variance structure on the logarithmic scale for each prefecture according to Mahalanobis distances of each age between 0 and 100 (Kim, 2000). Specifically, we consider a sequence of 2×1 vectors $\{\mathbf{x}_u = (\log[\text{Var}(\mathcal{Y}_t(u))], \log[E(\mathcal{Y}_t(u))])^\top; u = 0, \dots, 100\}$, and define the Mahalanobis distance of \mathbf{x}_u from its mean vector $\boldsymbol{\mu}$ as

$$\text{MD} = \sqrt{(\mathbf{x}_u - \boldsymbol{\mu})^\top \boldsymbol{\Sigma}^{-1} (\mathbf{x}_u - \boldsymbol{\mu})},$$

where $\boldsymbol{\Sigma}$ is the covariance matrix of \mathbf{x}_u . The Mahalanobis distance has an advantage over the commonly used Euclidean distance in identifying outliers in a collection of vectors like \mathbf{x}_u as the Mahalanobis distance reflects correlations among components of \mathbf{x}_u . Using a cut-off value obtained from the chi-square distribution $\chi_{0.95, \text{df}=2}^2$, we identify outlying pairs of $(\log[\text{Var}(\mathcal{Y}_t(u))], \log[E(\mathcal{Y}_t(u))])$ for any particular age u in some prefectures when applying the linear temporal TL, as shown in Figure A2 in the supplementary document. Nearly all identified outliers are related to age intervals with the lowest number of observed deaths (i.e. $8 \leq u \leq 12$ and $u \geq 95$). Prefectures that experienced relatively large variations of observed deaths at these ages between 1975 and 2018 may report large estimated temporal variances, contributing to the identified temporal outlying pairs of $(\log[\text{Var}(\mathcal{Y}_t(u))], \log[E(\mathcal{Y}_t(u))])$. In contrast, no outliers are detected for the years 1975–2018 for the linear spatial TL specification (Figure A1 in the supplementary document). This is because averaging all 44 prefectures smooths out influences of abruptly abnormal observed deaths in any given year.

Observations inflating the variance of both components of \mathbf{x}_u but having little influence on the correlation (i.e. in regression diagnostics, observations with large leverage but small residuals) may be reported with Mahalanobis distances slightly larger than the cut-off (see, e.g. section 4 of Kim, 2000). We exclude an observation from the identified outliers if its studentized residual (see, e.g. Faraway, 2014, for definition) is smaller than the critical value $t_{0.95, \text{df}=99}$, where $\text{df} = 99$ is the difference between the number of observations (101) and the number of estimated parameters (2) in the linear TL.

3 | EXTENSIONS OF TL ESTIMATION

3.1 | Cubic TL specification

To check for a potential nonlinear relationship between the $\log [\text{Var}(P)]$ and $\log [E(P)]$, Taylor et al. (1978) considered a quadratic TL:

$$\log[\text{Var}(P)] = \log a_2 + b_2 \cdot \log[E(P)] + c_2 \cdot \{\log[E(P)]\}^2 + \epsilon. \tag{4}$$

Xu and Cohen (2019) showed that the quadratic extension of the TL model described the spatial and temporal variation of US county population abundance better than the linear TL specification of (1). From Figure 2, children and teenagers (age less than 20), middle-aged adults (age between 30 and 50) and older people (age greater than 65) in a given prefecture may have different mortality patterns relative to the national average. In addition, a few prefectures report mortality rates closely following the national average in every year between 1975 and 2018, while some prefectures observe periodic fluctuations or abrupt changes in male mortality rates. Given the complex patterns of temporal and spatial variances of mortality rates across various ages, we further extend the quadratic TL to include a cubic term:

$$\log[\text{Var}(P)] = \log a_3 + b_3 \cdot \log[E(P)] + c_3 \cdot \{\log[E(P)]\}^2 + d_3 \cdot \{\log[E(P)]\}^3 + \epsilon. \tag{5}$$

We conduct the standard *t*-tests to check if estimated coefficients are significantly different from zero. When the *p*-value of a coefficient is less than 0.05 or, after Bonferroni correction, the *p*-value is less than 0.05/number of tests, the estimate is considered as significant. If the coefficient $d_3 \neq 0$, then the cubic extension (5) of TL model is deemed most appropriate for describing the mean-variance relationship. When d_3 is not significant but a fitted quadratic TL yields a significant c_2 , then we consider the quadratic TL as a suitable description of the mean-variance relationship. If the slope coefficient *b* in Equation (1) is significant and all c_2 , c_3 and d_3 are insignificant, the linear TL is considered as a suitable model of the relationship between $\log [\text{Var}(P)]$ and $\log [E(P)]$.

We estimate coefficients and associated standard errors of the linear TL (1) (*a* and *b*), the quadratic TL (4) (a_2 , b_2 and c_2), and the cubic TL (5) (a_3 , b_3 , c_3 and d_3), and also *p*-values corresponding to each estimate. We also recorded the adjusted coefficient of determination (adj. R^2) for each of the fitted OLS TL and extended TL models. The $(1 - \text{adj. } R^2)$ value of the preferred model (TL, quadratic TL or cubic TL) can be viewed as a measure of dissimilarity of age-specific mortality rates among spatial or temporal units relative to the standard of the linear function (1), the quadratic function (4), or the cubic function (5). Specifically, higher values of $(1 - \text{adj. } R^2)$ for the spatial TL (linear, quadratic or cubic) indicate larger dissimilarity from the standard specification in the spatial distribution of subnational age-specific mortality rates of Japan. Similarly, for the temporal TL (linear, quadratic or cubic), greater $(1 - \text{adj. } R^2)$ reflects larger dissimilarity from the standard specification in the temporal distribution of mortality rates within each prefecture.

3.2 | Robust estimation of the slope parameter

Figure 2 shows exceptionally high mortality rates in particular prefectures due to disasters such as earthquakes and tsunamis. Given that the OLS estimator is vulnerable to outliers in the mean

and variance statistics, unusual mortality observations can significantly affect the OLS estimate of the TL slope parameter.

We improve the robustness of estimating the slope parameter by considering the M -estimate. In the robust statistics literature, the efficiency and the breakdown point are two commonly used criteria to assess and compare various robust methods (see Donoho & Huber, 1983). The efficiency is used to measure the relative efficiency of a robust estimator compared to the OLS estimators when the error distribution is Gaussian and errors are free of outliers. In contrast, the breakdown point measures the proportion of outliers an estimate can tolerate before the estimated value goes to infinity.

In the robust estimation, we estimate TL coefficients simultaneously by solving optimization problems. Specifically, using the linear specification of (1) as a example, we search for \hat{a} and \hat{b} that minimize the objective function given by

$$\sum_u \rho \left\{ \frac{\log[\text{Var}(\mathcal{Y}_t(u))] - \log a - b \cdot \log[E(\mathcal{Y}_t(u))]}{\sigma} \right\}, \quad (6)$$

where $\rho(\cdot)$ is a robust loss function, and σ is an error scale estimate. In this paper, we first consider the most commonly used robust loss functions, namely the three-part loss function of Hampel (1974) given by

$$\rho(x) = \begin{cases} x & \text{for } 0 \leq |x| \leq p \\ p \text{ sign}(x) & \text{for } p \leq |x| \leq q \\ \frac{p(r-|x|)}{r-q} & \text{for } q \leq |x| \leq r \\ 0 & \text{for } r \leq |x| \end{cases},$$

with parameters $p = 1.5k$, $q = 3.5k$, and $r = 8k$ and $k = 0.9016$ for 95% efficiency. It is easy to see that the Hampel's robust loss function has two flat segments (i.e. $p \leq |x| \leq q$) and is not smooth at several places (i.e. $x = |p|, |q|$ or $|r|$). To retain the smoothness of functional data, we also consider the Tukey's bisquare loss function, given by

$$\rho(x) = \begin{cases} x \left(1 - \frac{x^2}{p^2}\right)^2 & \text{for } |x| \leq p \\ 0 & \text{for } |x| > p \end{cases},$$

which is smooth and continuous over the entire range of x . When $p = 4.685$, Tukey's bisquare function produces 95% efficiency (Hoaglin et al., 1983).

Using generic notations of mean and variance of age-specific mortality as well as the linear specification of (1), the estimation procedure for the spatial TL slope parameter can be summarized as follows:

Step 1 Use the OLS method to estimate parameters (\hat{a}, \hat{b}) .

Step 2 Calculate residual values $\epsilon_t = \log[\text{Var}(\mathcal{Y}_t(u))] - \log \hat{a} - \hat{b} \cdot \log E[\mathcal{Y}_t(u)]$ for $t = 1, 2, \dots, T$.

Step 3 Calculate error scale estimate $\hat{\sigma}_t = 1.4826 \times \text{MAD}$, where $\text{MAD} = \text{median}|\epsilon_t - \text{median}(\epsilon_t)|$.

- Step 4 Calculate standardized residual values $u_t = \epsilon_t / \hat{\sigma}_t$.
- Step 5 Calculate the weighted value $w_t = \rho(u_t)$ with a selected robust loss function ρ .
- Step 6 Calculate \hat{a}_M and \hat{b}_M using weighted least squares (WLS) method with weights w_t .
- Step 7 Repeat Steps 2 to 6 above to obtain convergent TL coefficients \hat{a}_M and \hat{b}_M .

A robust temporal TL estimation procedure can be obtained easily by replacing the spatial mean $E[\mathcal{Y}_t(u)]$ and spatial variance $\text{Var}[\mathcal{Y}_t(u)]$ with the corresponding temporal definitions, and then computing the sample residuals $\{\epsilon_j, j = 1, \dots, N\}$ over the N regions instead.

3.3 | Spatial covariance

Empirical studies concerning spatial TL generally hypothesize that populations of interest are identically (but not necessarily independently) distributed with finite mean and variance. Population densities measured at geographically separated locations tend to be correlated, a phenomenon known as synchrony in ecology. Synchrony decreases the estimated TL slope parameters of insects such as flying aphids (Reuman et al., 2017) and mammals such as Hokkaido voles (Cohen & Saitoh, 2016). Human mortality rates also cluster among neighbouring countries (Carracedo et al., 2018) and neighbouring subnational regions (Turi & Grigsby-Toussaint, 2017; Yang et al., 2015). The spatial–temporal patterns indicate that estimation of TL coefficients for age-specific mortality rates should consider the spatial correlation of metropolitan areas with high population density.

Census results of Japan indicate that three major metropolitan areas (i.e. the Kanto, Chukyo, and Kinki urban areas) together have 51.9% of the nation’s over 126 million population, with 23.2% of the national total located in 12 major cities (Statistics Bureau Ministry of Internal Affairs and Communications, 2020). In the light of the urban–rural mortality differences in developed countries, such as Japan (see, e.g. Li et al., 1994; Woods, 2003), we propose a new version of TL that incorporates spatial covariance in estimating coefficients.

Moran’s I (Moran, 1950) has been commonly used to measure spatial correlation, returning a value close to 1 when characteristics at various locations appear to be positively correlated. However, the possibility of negative values makes Moran’s I not suitable to replace the variance on the left side of (1) because the logarithm of a negative quantity is complex, not real-valued. To overcome this issue, we modify the spatial autocorrelation measure of Geary (1954) to quantify the variance of mortality in year t as

$$C_t^{\text{spatial}}(u) = \frac{\sum_{i=1}^N \sum_{j=1}^N w_{ij} [\mathcal{Y}_t^i(u) - \mathcal{Y}_t^j(u)]^2}{2 \sum_{i=1}^N \sum_{j=1}^N w_{ij}}, \quad i, j = 1, \dots, N, \tag{7}$$

where w_{ij} is a matrix of spatial weights with zeros on the diagonal (i.e. $w_{ii} = 0$) and with the reciprocal of distance (in kilometres) between prefectures i and j as the remaining elements, that is $w_{ij} = 1/\text{distance}_{ij}$ for $i \neq j$. Using the Geosphere package (Hijmans, 2019) in **R**, the distance between any two prefectures is computed according to the longitude and latitude coordinates (World Cities Database, 2021) of their capital cities that host the majority of the population. The spatial variance $C_t^{\text{spatial}}(u)$ can replace the variance definition $\text{Var}_{\text{Spatial}}[\mathcal{Y}_t(u)]$ in the conventional spatial TL estimation (where identical distributions for the considered regional populations are assumed), taking account of distances between regions in the TL estimation.

3.4 | Long-run variance

In statistics, the long-run covariance enjoys a vast literature in the case of finite-dimensional time series, since the seminal work of Bartlett (1946) and Parzen (1957). The long-run covariance is still the most commonly used technique for smoothing the periodogram by employing a smoothing weight function and a bandwidth parameter. In functional time series, long-run covariance plays an important role in inference and modelling temporal dependence (see, e.g. Hörmann et al., 2015; Kokoszka et al., 2017; Li et al., 2020; Rice & Shang, 2017). Most early applications of the long-run covariance in the literature concern stationary functional time series (see, e.g. Hörmann et al., 2015; Shang, 2019), whereas recent research relaxes the stationarity assumption (see, e.g. Martínez-Hernández et al., 2020).

The long-run covariance has also been tested to work on a finite collection of age-specific mortality functions (see, e.g. Gao et al., 2019). Since our focus is accounting for long-run temporal dependence in the application of TL to age-specific mortality functions, we compute a long-run variance function $C^j(u)$, which can be viewed as the long-run covariance without cross-age dependence, for series related to region j as

$$C^j(u) = \sum_{\ell=-\infty}^{\infty} \gamma_{\ell}^j(u) = \sum_{\ell=-\infty}^{\infty} \text{cov}[\mathcal{Y}_t^j(u), \mathcal{Y}_{t+\ell}^j(u)], \quad u \in [0, 100], \quad (8)$$

where ℓ represents time lags of functions. From Equation (8), $C^j(u)$ is independent of t , thus the long-run variance function assumes stationarity. Replacing the robust temporal TL estimation of (6) by the long-run variance $C^j(u)$ enables consideration of the potential serial dependence of mortality functions assuming no dependence across ages.

The long-run variance function $C^j(u)$ can be estimated from a finite sample of functional objects $\{\mathcal{Y}_t^j(u), t = 1, \dots, T\}$ by a kernel sandwich estimator (Andrews, 1991) defined as

$$\hat{C}_{h,q}^j(u) = \sum_{\ell=-\infty}^{\infty} W_q\left(\frac{\ell}{h}\right) \hat{\gamma}_{\ell}^j(u), \quad (9)$$

where h is called the bandwidth parameter, and the estimator of $\gamma_{\ell}^j(u)$ is defined by

$$\hat{\gamma}_{\ell}^j(u) = \begin{cases} \frac{1}{T} \sum_{t=1}^{T-\ell} \left[\mathcal{Y}_t^j(u) - \frac{1}{T} \sum_{t=1}^T \mathcal{Y}_t^j(u) \right] \left[\mathcal{Y}_{t+\ell}^j(u) - \frac{1}{T} \sum_{t=1}^T \mathcal{Y}_t^j(u) \right], & \ell \geq 0; \\ \frac{1}{T} \sum_{t=1-\ell}^T \left[\mathcal{Y}_t^j(u) - \frac{1}{T} \sum_{t=1}^T \mathcal{Y}_t^j(u) \right] \left[\mathcal{Y}_{t+\ell}^j(u) - \frac{1}{T} \sum_{t=1}^T \mathcal{Y}_t^j(u) \right], & \ell < 0. \end{cases}$$

$W_q(\cdot)$ in Equation (9) is a continuous and symmetric weight function with bounded support of order q defined on $[-m, m]$ for some $m > 0$ satisfying

$$W_q(0) = 1, W_q(u) \leq 1, W_q(u) = W_q(-u), W_q(u) = 0 \text{ if } |u| > m.$$

The weight function W_q also satisfies

$$0 < \lim_{u \rightarrow 0} |u|^{-q} (1 - W_q(u)) < \infty.$$

As with the kernel sandwich estimator in Equation (9), the crucial part is the estimation of bandwidth parameter h . We estimate h through a data-driven approach using the plug-in

algorithm of Rice and Shang (2017, section 2). The plug-in algorithm selects the optimal bandwidth h that minimizes the asymptotic mean-squared normed error between the estimated and actual long-run variance functions.

3.5 | Long-run spatial variance

To consider both temporal and spatial dependence simultaneously, we combine the long-run covariance (8) focusing on correlation of observed measurements over time with the spatial variance (7) focusing on correlation of observed measurements over space, and compute a long-run spatial variance $C^{LR\text{spatial}}$ as

$$C^{LR\text{spatial}}(u) = \sum_{\ell=-\infty}^{\infty} \left(\theta \cdot C_{t+\ell}^{\text{spatial}}(u) + (1 - \theta) \sum_{j=1}^N \gamma_{\ell}^j(u) \right), \tag{10}$$

where $\theta \in [0, 1]$ is a weight balancing the spatial and temporal components of $C^{LR\text{spatial}}(u)$.

The long-run spatial variance of (10) has the conventional long-run variance of (8) and the spatial variance of (7) as its special cases, and as a consequence, simultaneously incorporates spatial and temporal correlations of subnational mortality rates in various regions. We are interested in temporal and spatial variances of mortality rates of the population at a given age u as in Equations (2) and (3). Thus, measuring the dependence of mortality rates between different age groups is out of the scope of (10).

Via a kernel estimator similar to Equation (9), the long-run spatial variance can be estimated as

$$\hat{C}^{LR\text{spatial}}(u) = \sum_{\ell=-\infty}^{\infty} W_q \left(\frac{\ell}{h} \right) \left(\vartheta \cdot \frac{\sum_{i=1}^N \sum_{j=1}^N w_{ij} \left(\mathcal{Y}_t^i(u) - \mathcal{Y}_{t+\ell}^j(u) \right)^2}{2 \sum_{i=1}^N \sum_{j=1}^N w_{ij}} + (1 - \vartheta) \hat{\gamma}_{\ell}^j(u) \right), \tag{11}$$

where the optimal ϑ in practice can be selected to give the best model-fitting result or forecasting performance, for example the smallest sample-size adjusted Akaike information criterion (AICc) or the highest predicted R^2 .

4 | RESULTS

4.1 | Confirmation of TL specifications

We first compare model fitting performances of the linear TL (1) with the proposed quadratic TL (4) and cubic (5) on the total, female and male series of subnational age-specific mortality rates in Japan. We consider all observations without excluding any outliers in this step of model comparison. Table 1 summarizes the averaged regression statistics of the fitted linear and non-linear TL models, including the adjusted coefficient of determination (adj. R^2), the AICc information criterion, and the number of estimated coefficients significantly different from 0 before and after Bonferroni correction.

As expected, the fitted cubic TL models give the highest adj. R^2 among all considered TL specifications. A larger adj. R^2 value means explanatory variables explain more variation in the

TABLE 1 Summary of the regression statistics of the linear TL (Equation 1) and its quadratic (Equation 4) and cubic (Equation 5) extensions using subnational age-specific mortality rates in Japan

	Total series			Female series			Male series		
	Linear	Quadratic	Cubic	Linear	Quadratic	Cubic	Linear	Quadratic	Cubic
Spatial TL (Number of tests = 44)									
Mean adj. R^2	0.9610	0.9894	0.9940	0.9575	0.9896	0.9932	0.9432	0.9796	0.9914
Mean AICc	52.3348	-77.8971	-135.4642	58.5237	-83.0680	-125.8049	95.8324	-6.3794	-91.8324
Significant \hat{b}	44/44	44/44	44/44	44/44	44/44	44/44	44/44	44/44	44/44
Significant \hat{c}	-	44/44	44/44	-	44/44	44/44	-	44/44	44/44
Significant \hat{d}	-	-	43/44	-	-	43/44	-	-	44/44
Bonferroni \hat{b}	44/44	44/44	44/44	44/44	44/44	44/44	44/44	44/44	44/44
Bonferroni \hat{c}	-	44/44	43/44	-	44/44	43/44	-	44/44	44/44
Bonferroni \hat{d}	-	-	43/44	-	-	43/44	-	-	44/44
Temporal TL (Number of tests = 47)									
Mean adj. R^2	0.9838	0.9908	0.9938	0.9851	0.9907	0.9949	0.9770	0.9906	0.9910
Mean AICc	74.6309	69.7221	22.9991	77.6934	74.1325	0.9916	66.5033	57.7928	36.2515
Significant \hat{b}	47/47	47/47	43/47	47/47	47/47	33/47	47/47	47/47	47/47
Significant \hat{c}	-	47/47	43/47	-	46/47	47/47	-	47/47	25/47
Significant \hat{d}	-	-	45/47	-	-	47/47	-	-	22/47
Bonferroni \hat{b}	47/47	47/47	36/47	47/47	47/47	28/47	47/47	47/47	47/47
Bonferroni \hat{c}	-	46/47	37/47	-	43/47	44/47	-	47/47	16/47
Bonferroni \hat{d}	-	-	43/47	-	-	47/47	-	-	6/47

response variable after adjusting for the increased number of predictors. Almost all estimated coefficients of the fitted quadratic and cubic spatial TL extensions are significantly different from 0, indicating that the cubic TL model is favoured over the linear TL model for analysing mortality data in the period 1975–2018. Similarly, under both temporal and spatial TL settings, the AICc for cubic specifications are estimated to be smaller than quadratic and linear TL settings for all three series. The lowest mean AICc scores indicate that cubic TL extensions are favoured in analysing both temporal correlation and spatial synchrony of mortality in Japan. Moreover, the cubic temporal TL model is favoured over the linear temporal TL model for all prefectures for female series and a majority of 47 prefectures for total series, regardless of Bonferroni correction. For the male series, the quadratic and cubic temporal TL models are preferred over the linear TL specification for about half of all prefectures before Bonferroni correction. In contrast, the linear model is preferred in more prefectures after Bonferroni correction of regression significance. Therefore, considering the high explanatory power and the overall regression significance, the cubic TL specification is selected as a ‘best fit’ function of variance-mean relationship on the log-log scale for Japan’s spatial and temporal subnational mortality rates. Figures A1 and A2 in the supplement illustrate the excellent fit of the spatial cubic TL model for yearly mortality data and the temporal TL model respectively for observations in each prefecture. In the remainder of this section, we mainly report the results of fitted cubic TL models.

4.2 | Weighted spatial TL

To apply the proposed spatial TL weighted by correlation among all 47 prefectures in Japan, we first locate the city with the largest population in every prefecture and define weights as reciprocal to distances (in kilometres) between the identified cities. Next, the spatial variance (7) is computed and regressed on the spatial mean (3) for spatial TL coefficients. Figure 3 shows the estimated coefficients of spatial TL in the cubic specification (5) for subnational total, female and male mortality series in Japan over 44 years from 1975 to 2018, obtained by the OLS estimation method and robust estimation methods with Hampel weights and bisquare weights.

The fitted spatial TL models and robust spatial TL models all report adj. R^2 averaged over 44 years over 0.99 (i.e. 0.9940 (OLS), 0.9940 (Hampel), 0.9937 (bisquare) for total series, 0.9932 (OLS), 0.9931 (Hampel), 0.9927 (bisquare) for female series, and 0.9914 (OLS), 0.9912 (Hampel), 0.9900 (bisquare) for male series), indicating that almost all variation in $\log(\text{spatial variance})$ of subnational mortality can be explained by the corresponding $\log(\text{spatial mean})$ values.

Apart from several $\hat{\alpha}_3$ for the male series, the remaining estimated spatial TL coefficients shown in Figure 3 are all significantly different from 0. Most robust TL parameter estimates, especially those obtained with bisquare weights, are much lower than the OLS estimates before 1990. We believe robust estimates produce lower estimated coefficients in a given year because a few ages have widely varying mortality rates across various prefectures in Japan, inflating spatial variances. Figure 4 shows that the ordinary spatial variance (as defined in Equation 7) of all series in 1985 grows steeply over age 60 in 1985. The increment of spatial variance for old ages is reduced gradually over time, which reflects converging mortality trends of rural and urban areas in Japan (e.g. Hao et al., 2012). These mortality trends are partly caused by rapid urbanization in the country since the 1970s, reducing socioeconomic and health inequality in subnational populations significantly (Fukuda et al., 2005). When regressing spatial variances of all ages between 0 and 100 on their spatial means, the robust estimation methods scale down impacts of

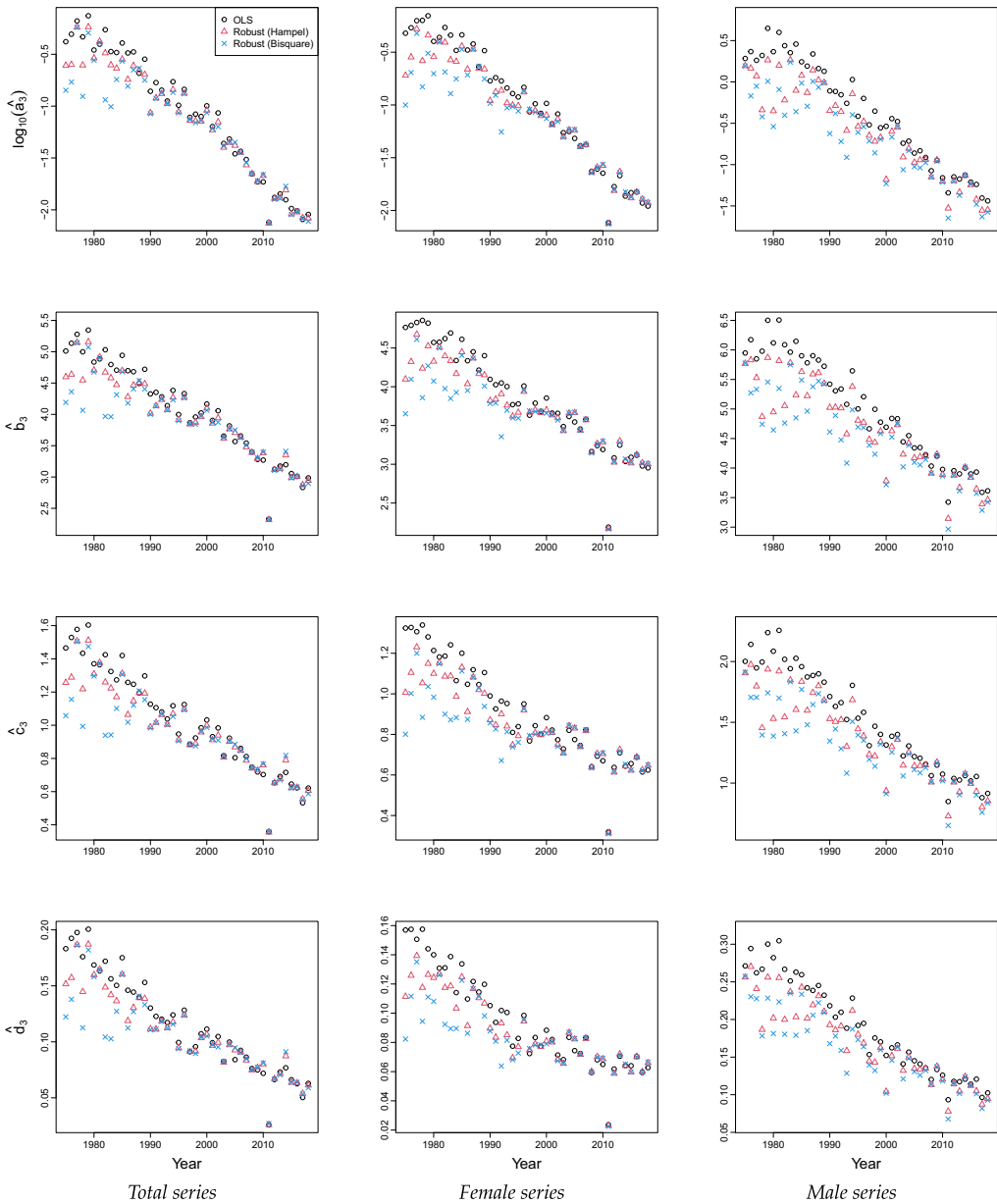


FIGURE 3 Estimated spatial TL coefficients for subnational mortality series in Japan from 1975 to 2018 (averaged over 47 prefectures). From top to bottom, four rows of scatter plots correspond to a_3 , b_3 , c_3 and d_3 of (5), respectively. [Colour figure can be viewed at wileyonlinelibrary.com]

observations with considerable spatial variances near the upper end of the mortality curve and thus give smaller estimated coefficients than the OLS method.

The surprisingly low spatial TL coefficient estimates in the year 2011 in Figure 3 relate to the Great East Japan earthquake and tsunami that caused nearly 20,000 deaths in Iwate, Miyagi, Fukushima prefectures, leading to increased mortality for both sexes (Nakahara & Ichikawa, 2013). The influence of natural disasters in 2011 on the spatial variance of mortality is more

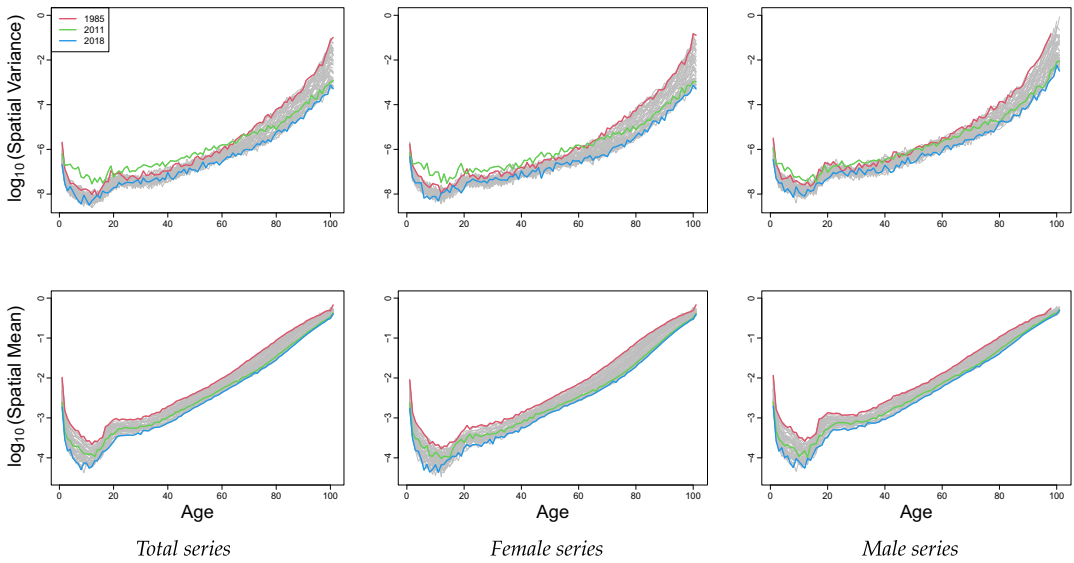


FIGURE 4 Ordinary spatial variance and spatial mean of subnational mortality in Japan (missing values in male series over 98–100 years of age). [Colour figure can be viewed at wileyonlinelibrary.com]

obvious for ages less than 60 (Figure 4). Since all victims are located in the north-eastern coastal prefectures, abnormally large mortality observations of the affected prefectures exaggerated weighted spatial variance of the whole country in 2011. Smaller spatial TL estimates \hat{a}_3 to \hat{d}_3 in a cubic log-regression form capture this year’s sudden increase in variance over the mean mortality range $\log(\text{mean}) \in (-4.02, -0.29)$. Spatial variances of male series fluctuate considerably (Figure 4): spatial variances in 1985 are higher than those in 2011 for some ages within the 20–50 range. The OLS estimation method is influenced by such outlying observations located far from the fitted cubic regression line. It thus gives inaccurate 2011 estimated coefficients that are not very different from other years. In contrast, the robust algorithm with Tukey’s bisquare weights yields distinctly lower estimated \hat{a}_3 to \hat{d}_3 , consistent with estimates for total series and female series in the same year. This empirical application indicates that the robust TL estimation methods can produce more reliable TL coefficients in the presence of outliers, contributing to more accurate TL-based statistical analysis and inference.

4.3 | Long-run temporal TL

Regressing the long-run variance of (9) on the temporal mean of (2) gives long-run temporal TL coefficients. Figure 5 shows long-run temporal TL estimates in the cubic specification (5) for Japanese subnational mortality series obtained by the OLS and the robust estimation methods. The robust estimation with bisquare weights generally gives the lowest estimates for regression intercepts and coefficients up to cubic orders. The total series and female series report small differences between parameters estimated by the OLS and robust methods. In contrast, the male series show significantly different OLS and bisquare robust estimates, reflecting large fluctuations of Japan male mortality before and after World War II (see, e.g. Jannetta & Preston, 1991, figure 4).

The long-run temporal TL coefficients estimated by the bisquare method tend to be lower than OLS estimates for female and male series in many prefectures (Figure 5). Using results for the

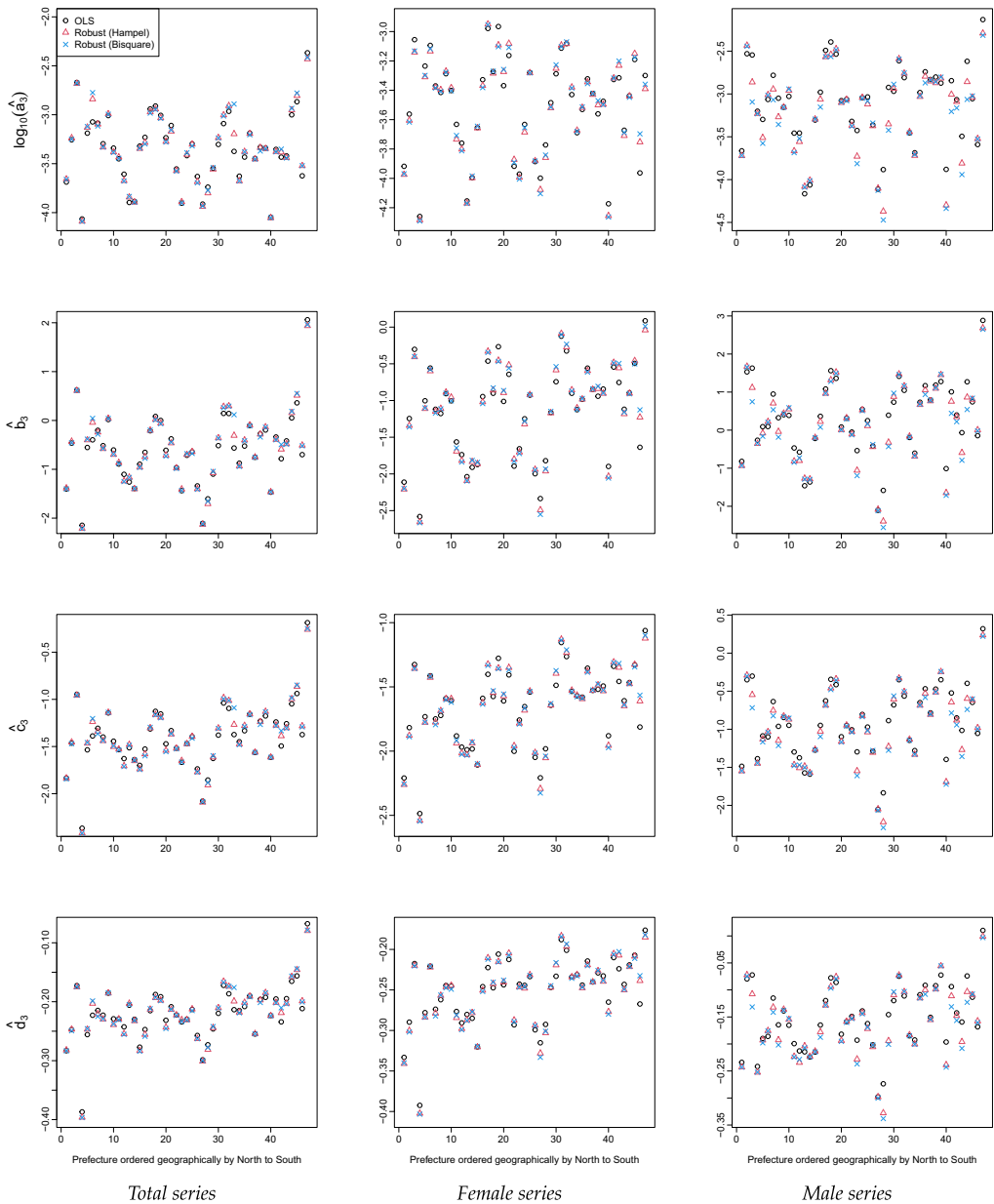


FIGURE 5 Estimated temporal TL coefficients for subnational Japanese mortality series from 1975 to 2018 (44 years). From top to bottom, four rows of scatter plots correspond to a_3 , b_3 , c_3 and d_3 of (5), respectively. [Colour figure can be viewed at wileyonlinelibrary.com]

male series as an example, two prefectures with the largest differences between OLS and bisquare coefficient estimates in Figure 5 are Hyōgo (28) and Iwate (3). Large reductions in the robust estimates are associated with Hyōgo and Iwate because the estimated long-run covariances of mortality are inflated by the large number of deaths related to natural disasters.

Males in Hyōgo have long-run temporal variances of mortality lower than most other male populations in Japan except for ages between 50 and 85 (Figure 6). High temporal variances of mortality for people over 50 in Hyōgo are due to the great Hanshin earthquake that occurred

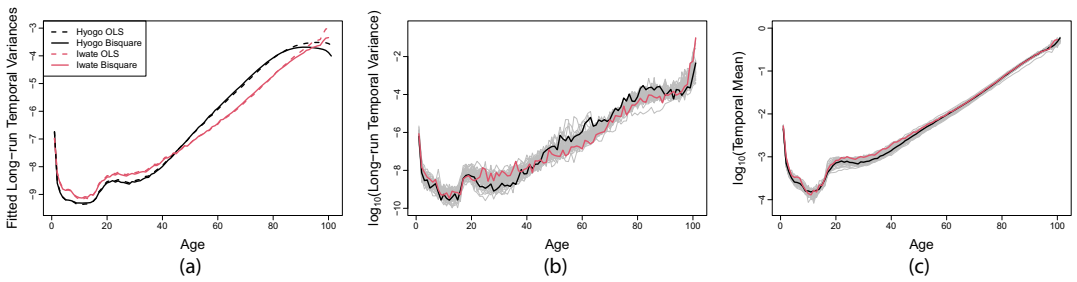


FIGURE 6 (a) Fitted TL models for male mortality series in Hyogo and Iwate between 1975 and 2018. (b) Empirical long-run temporal variance for ages between 0 and 100 used as the response in the fitted TL models. (c) Empirical temporal mean for ages between 0 and 100 used as predictors in the fitted TL models. [Colour figure can be viewed at [wileyonlinelibrary.com](https://onlinelibrary.wiley.com/doi/10.1111/rssa.12859)]

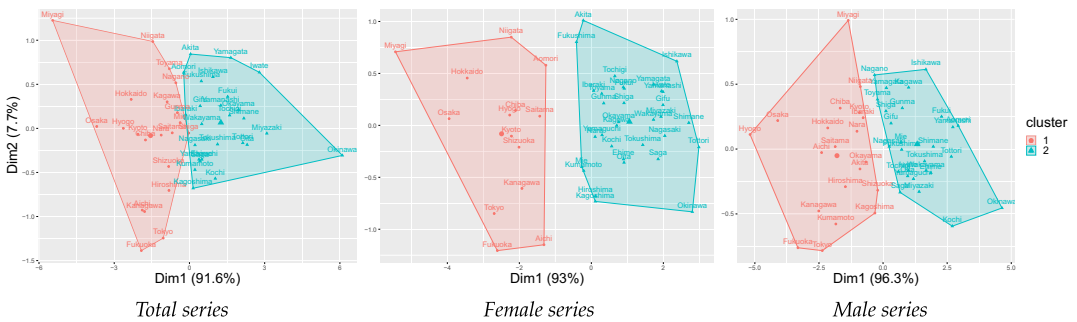


FIGURE 7 *K*-means clustering memberships of long-run temporal TL coefficients obtained by the robust method with bisquare weights. [Colour figure can be viewed at [wileyonlinelibrary.com](https://onlinelibrary.wiley.com/doi/10.1111/rssa.12859)]

near Kobe in 1995, which significantly affected older people. Specifically, more than 60% of 5,502 fatalities of the earthquake were among those over 60 years old, and surviving older people tended to be left behind as the most vulnerable after the disaster (Tanida, 1996). Similarly, Iwate suffered catastrophic damage in the massive tsunami in 2011 with exceptionally high casualties in people aged 65 and over (e.g. figure 2 in Nakahara & Ichikawa, 2013). The bisquare robust methods mitigate influences of ages with high temporal variances on the estimation of the overall TL curve, thus providing fitted temporal variances of mortality rates at elder ages much lower than those obtained by the OLS method.

Figure 5 demonstrates the high similarity between Hampel and bisquare long-run temporal TL estimates. Since we are interested in differences between robust long-run temporal TL estimates and the conventional OLS estimates, the following analysis compares bisquare long-run temporal TL estimates with OLS estimates. To further analyse the long-run temporal TL coefficient estimates, we apply *K*-means clustering via principal component analysis (see, e.g. Ding & He, 2004). We cluster the estimated long-run temporal TL coefficients into two groups based on the total within-cluster sum of squares (shown in Figure A3 in the supplement) for the total, female, and male series. For example, clustering results of bisquare long-run TL coefficients are illustrated in Figure 7.

The first principal component capturing the largest variance of the long-run temporal TL coefficient estimates is considered a new variable ‘Dimension 1’ (or ‘Dim 1’). In contrast, the second principal component is ‘Dimension 2’ (or ‘Dim 2’). In Figure 7, all prefectures

grouped into Cluster 1 have negative values for Dimension 1 whereas a large majority of prefectures belonging to Cluster 2 have positive Dimension 1 values. Cluster 1 covers 15 of 17 prefectures in the megalopolis known as the Taiheiyō Belt in Japan (see, e.g. Bienvenido-Huertas et al., 2020). In particular, all 9 prefectures in the roughly continuous urban Tokyo-Nagoya-Osaka strip can be found in Cluster 1 for all three series. Hence, Dimension 1 differentiates prefectures with high economic output from the rest (presented in detail in Table 2).

Long-run temporal TL coefficients obtained by OLS and robust methods are strongly positively correlated with Dimension 1 (Figure 8). Miyagi is highlighted to have the lowest estimated TL coefficients for total and female series, while Hyōgo and Osaka are identified to have the lowest TL estimates for male series. These three prefectures all experienced sudden increases in mortality due to earthquakes and tsunami (Nakahara & Ichikawa, 2013; Tanida, 1996). Okinawa has the highest TL estimates for all three series, probably due to the exceptional longevity in the prefecture (Poulain, 2011). Hence, Dimension 1, constructed as a linear projection of long-run temporal TL coefficients, can effectively distinguish populations enjoying low mortality consistently throughout 1975–2018 from those influenced by natural disasters.

The socioeconomic status of a community is substantially associated with its mortality (see, e.g. Anderson et al., 1997; Ben-Shlomo et al., 1996; Fukuda et al., 2005). Hence, we compare Japan's ranking of prefectures by total gross domestic product (GDP) and GDP per capita (GDPPP) in 2016 published by OECD (2020) with detailed clustering memberships (Table 2). Fifteen prefectures have both their females and males grouped into the Cluster 1 based on bisquare TL estimates, whereas 23 prefectures have both females and males grouped into the Cluster 2 based on bisquare TL estimates. Thus, females and males in 38 of 47 prefectures are assigned to concordant clusters based on bisquare estimates of cubic long-run temporal TL parameters. In contrast, according to the OLS long-run temporal TL coefficients, only nine prefectures have female and male series classified into the same cluster. Also, prefectures ranked between 1 and 22 by GDP have most of their total, female and male series classified into the first cluster. In contrast, prefectures ranked lower than Gifu (21) by GDP have almost all mortality series grouped into the second cluster. Highly consistent patterns between clustering results based on bisquare estimates and GDP rankings confirm the hypothesis that economic activity is strongly associated with mortality decline in post-war Japan (see, e.g. Tapia Granados, 2008). Estimating long-run temporal TL coefficients with bisquare weights reduces the influences of unusual observations caused by natural disasters, providing better estimates than the conventional OLS method.

Compared with GDP rankings, GDPPP rankings of prefectures match clustering results based on either estimation method much more poorly. This is not surprising since rankings of health expenditure per capita in Japan do not strictly follow the ordering of prefectural GDPPP, for example Hokkaido (GDPPP ¥ 34,579,100) and Yamaguchi (GDPPP ¥ 40,002,100) reported more real health-care expenditure per capita between 2001 and 2010 than Tokyo (GDPPP ¥ 75,456,500) (Tamakoshi & Hamori, 2015). We compute odds ratios quantifying the strength of association between GDP and GDPPP rankings and clustering results based on long-run temporal TL estimates. Figure 7 shows 22, 17, and 22 prefectures in Cluster 1 for the total series, the female series and the male series, respectively. To test whether prefectures in Cluster 1 also have high economic output, for the total and male series we assign a label 'High' to the first 22 prefectures ranked by GDP or GDPPP, and for the female series we assign a label 'High' to the first 17 prefectures ranked by GDP or GDPPP; we label all the remaining prefectures as 'Low'. The

TABLE 2 Japanese prefectures ranked by 2016 total GDP (in Million ¥) and GDPPP (in ¥), with clustering memberships based on long-run temporal TL coefficient estimates

Prefecture (Index)	GDP (Million ¥)	GDP Ranking	GDPPP (¥)	GDPPP Ranking	Bisquare Cluster			OLS Cluster		
					Total	Female	Male	Total	Female	Male
Tokyo (13)	104,470,000	1	7,668,090	1	1	1	1	1	1	1
Aichi (23)	39,409,400	2	5,249,690	2	1	1	1	1	1	1
Osaka (27)	38,995,000	3	4,414,690	8	1	1	1	1	1	1
Kanagawa (14)	34,609,300	4	3,784,510	26	1	1	1	1	1	1
Saitama (11)	22,689,700	5	3,112,870	45	1	1	1	1	1	1
Hyogo (28)	20,937,800	6	3,793,080	25	1	1	1	1	1	1
Chiba (12)	20,391,600	7	3,269,980	44	1	1	1	1	1	1
Fukuoka (40)	19,144,000	8	3,750,790	29	1	1	1	1	1	1
Hokkaido (1)	19,018,100	9	3,553,460	34	1	1	1	1	1	1
Shizuoka (22)	17,044,400	10	4,621,580	3	1	1	1	1	1	1
Ibaraki (8)	13,056,700	11	4,494,570	7	1	1	2	1	1	1
Hiroshima (34)	11,944,700	12	4,210,320	12	1	2	2	2	1	1
Kyoto (26)	10,487,600	13	4,025,930	18	1	1	1	1	1	1
Miyagi (4)	9,475,480	14	4,066,730	16	1	2	1	1	1	1
Tochigi (9)	8,958,400	15	4,556,660	4	2	1	2	2	2	1
Niigata (15)	8,883,970	16	3,886,250	23	1	1	1	1	1	1
Gunma (10)	8,528,500	17	4,335,790	10	1	2	2	1	2	1
Nagano (20)	8,272,260	18	3,961,810	21	1	1	1	1	1	1
Mie (24)	8,220,910	19	4,546,960	5	1	2	1	2	1	1
Fukushima (7)	7,917,870	20	4,165,110	13	2	1	1	1	1	2
Okayama (33)	7,681,160	21	4,011,050	20	1	2	2	1	1	1
Gifu (21)	7,621,800	22	3,769,440	27	2	1	1	2	2	1
Shiga (25)	6,381,690	23	4,516,420	6	2	2	1	2	2	1
Yamaguchi (35)	6,087,530	24	4,366,950	9	2	2	2	2	1	2
Kumamoto (43)	5,927,630	25	3,341,390	40	1	2	1	1	1	1
Kagoshima (46)	5,381,810	26	3,287,610	42	2	2	2	1	1	1
Ehime (38)	5,074,180	27	3,690,310	30	2	2	2	2	2	2
Iwate (3)	4,674,260	28	3,686,320	31	2	2	2	2	2	2
Ishikawa (17)	4,623,030	29	4,016,530	19	2	2	2	2	2	2
Aomori (2)	4,580,260	30	3,542,350	35	2	2	2	2	2	2
Toyama (16)	4,566,280	31	4,303,760	11	1	2	2	2	2	1
Nagasaki (42)	4,566,160	32	3,340,280	41	2	2	2	2	2	2
Oita (44)	4,353,380	33	3,752,920	28	2	2	1	2	2	2

(Continues)

TABLE 2 (Continued)

Prefecture (Index)	GDP (Million ¥)	GDP Ranking	GDPPP (¥)	GDPPP Ranking	Bisquare Cluster			OLS Cluster		
					Total	Female	Male	Total	Female	Male
Okinawa (47)	4,281,960	34	2,975,650	46	2	2	2	2	2	2
Yamagata (6)	4,039,810	35	3,629,660	33	2	2	1	2	2	1
Kagawa (37)	3,802,230	36	3,911,760	22	2	2	2	2	2	2
Miyazaki (45)	3,683,970	37	3,361,280	38	2	2	2	2	2	2
Wakayama (30)	3,676,470	38	3,853,740	24	2	2	2	2	2	2
Nara (29)	3,650,720	39	2,692,270	47	1	2	2	2	2	2
Akita (5)	3,451,340	40	3,417,160	37	2	2	2	2	2	1
Yamanashi (19)	3,365,640	41	4,054,980	17	2	2	2	2	2	2
Fukui (18)	3,211,130	42	4,106,310	14	2	2	2	2	2	2
Tokushima (36)	3,071,970	43	4,095,960	15	2	2	2	2	2	2
Saga (41)	2,851,910	44	3,444,340	36	2	2	2	2	2	2
Shimane (32)	2,520,650	45	3,653,110	32	2	2	2	2	2	2
Kochi (39)	2,419,430	46	3,355,660	39	2	2	2	2	2	2
Tottori (31)	1,864,070	47	3,270,300	43	2	2	2	2	2	2

numbers of prefectures with ‘High’ and ‘Low’ labels in Clusters 1 and 2 are then organized into 2×2 tables (Table 3). Odds ratios of GDP and GDPPP rankings are computed following the standard method for contingency tables. In Table 3, the larger empirical odds ratios indicate stronger associations between clustering memberships and rankings (by GDP or GDPPP). For female series, clustering memberships based on bisquare estimates are seen to have the highest association with total GDP rankings of prefectures, as indicated by an odds ratio of 42.00. For male and total series, clustering memberships based on OLS estimates are seen to have the strongest association with total GDP rankings, as indicated by odds ratios of 115.00 and 66.50, respectively. In summary, clustering results based on long-run temporal TL coefficient estimates have stronger associations with prefectural total GDP rankings, confirming that sub-national mortality rates in Japan are substantially associated with the economic status of each prefecture.

4.4 | Spatial-temporal TL

We combine spatial and temporal information of Japanese subnational age-specific mortality rates to compute the long-run spatial-temporal variance $C^{LR\text{spatial}}$ according to Equation (11). Then we regress the logarithm of $C^{LR\text{spatial}}$ on the logarithm of overall mean mortality averaged over space and time as $E_{\text{overall}} = (NT)^{-1} \sum_{t=1}^T \sum_{j=1}^N \mathcal{Y}_t^j(u)$ for long-run spatial-temporal TL coefficients. Table 4 summarizes regression statistics of long-run spatial-temporal TL under the cubic specification of (5). Apart from the \hat{c}_3 obtained by the OLS method

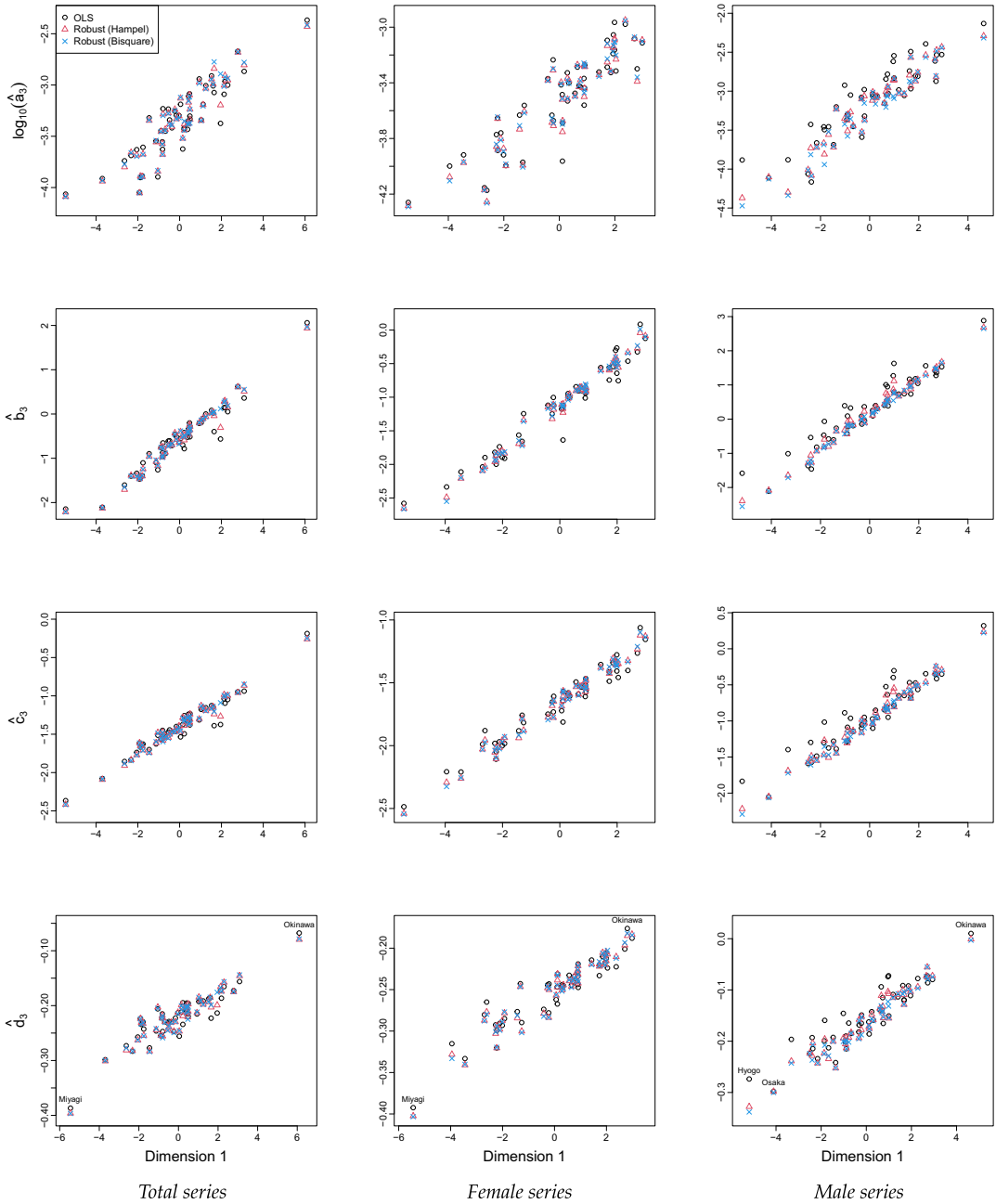


FIGURE 8 Estimated temporal TL coefficients (averaged over 1975–2018) against Dimension 1 of k -means clustering results shown in Figure 7. [Colour figure can be viewed at wileyonlinelibrary.com]

TABLE 3 Odds ratios quantifying association between clustering results based on long-run temporal TL coefficient estimates and prefecture rankings based on indicators of economic activity

Series	Cluster	GDP		Odds ratio	GDPPP		Odds ratio
		High	Low		High	Low	
Bisquare cluster							
Total	1	19	3	46.44	13	9	2.57
	2	3	22		9	16	
Female	1	14	3	42.00	7	10	1.40
	2	3	27		10	20	
Male	1	18	4	23.62	11	11	1.27
	2	4	21		11	14	
OLS cluster							
Total	1	20	2	115.00	13	9	2.57
	2	2	23		9	16	
Female	1	15	5	37.50	8	12	1.33
	2	2	25		9	18	
Male	1	21	6	66.50	15	12	2.32
	2	1	19		7	13	

for males, all the remaining regression coefficients are highly significant at 95% confidence levels. Minimal differences can be observed in fitted long-run spatial-temporal TL regressions obtained by OLS and robust estimation methods for particular mortality series (Figure 9).

In Table 4 and Figure 9, we report a selection of weighting coefficients $\theta = 0.05, 0.50, 0.95$. Fitting results of other possible weights are included in Figure A4 in the supplement. The choice of $\theta = 0.05$ corresponds to $\hat{C}^{LR\text{spatial}}$ focusing mostly on temporal variation of the considered mortality series, whereas $\theta = 0.95$ concentrates on spatial differences of mortality. For any particular series and estimation method, it can be seen that at $\theta = 0.95$ the smallest AICc is reached while the largest predicted R^2 is also achieved. Thus, the spatial variance component in Equation (11) dominates the temporal variance component in the optimal long-run spatial-temporal TL.

In addition to the cubic TL specification, we further apply the conventional linear TL specification (1) to analyse the estimated long-run spatial-temporal TL. All linear spatial-temporal TL slope estimates for female, male and total series fall in the interval [1.75, 1.88], confirming the range of [1, 2] for human TL slopes based on population density and age-specific mortality rates (Bohk et al., 2015; Xu & Cohen, 2019) and for the population density or population sizes of many non-human animals and plants (Anderson et al., 1982). The high predicted R^2 of the fitted models suggests excellent explanatory power of linear TL regressions. Thus, the proposed long-run spatial-temporal TL can summarize spatial and temporal changes in human mortality rates in a single coefficient that is straightforward to use in practice.

TABLE 4 Summary of regression statistics of cubic long-run spatial-temporal TL using age-specific mortality rates in Japan from 1975 to 2018

	$\theta = 0.05$			$\theta = 0.50$			$\theta = 0.95$		
	OLS	Hampel	Bisquare	OLS	Hampel	Bisquare	OLS	Hampel	Bisquare
Total Series									
$\log_{10}(\hat{a}_3)$	-1.2609*	-1.3001*	-1.3216*	-1.5394*	-1.5786*	-1.6001*	-2.5351*	-2.5743*	-2.5961*
\hat{b}_3	0.6505*	0.5546*	0.5133*	0.6508*	0.5551*	0.5137*	0.6581*	0.5623*	0.5207*
\hat{c}_3	-0.7787*	-0.8379*	-0.8570*	-0.7785*	-0.8377*	-0.8568*	-0.7752*	-0.8345*	-0.8536*
\hat{d}_3	-0.1344*	-0.1436*	-0.1459*	-0.1344*	-0.1436*	-0.1458*	-0.1340*	-0.1432*	-0.1454*
AICc	-90.5929	-87.3026	-85.4916	-90.6155	-87.3270	-85.5137	-91.0412	-87.7587	-85.9296
Pred. R^2	0.9939	0.9935	0.9930	0.9939	0.9935	0.9930	0.9940	0.9935	0.9930
Female Series									
$\log_{10}(\hat{a}_3)$	-1.1548*	-1.1908*	-1.2074*	-1.4333*	-1.4693*	-1.4859*	-2.4281*	-2.4643*	-2.4807*
\hat{b}_3	0.6494*	0.5592*	0.5260*	0.6499*	0.5597*	0.5265*	0.6591*	0.5687*	0.5360*
\hat{c}_3	-0.9066*	-0.9644*	-0.9819*	-0.9064*	-0.9642*	-0.9817*	-0.9021*	-0.9599*	-0.9772*
\hat{d}_3	-0.1653*	-0.1744*	-0.1770*	-0.1652*	-0.1744*	-0.1769*	-0.1647*	-0.1738*	-0.1764*
AICc	-81.2292	-78.1845	-77.4999	-81.2496	-78.2059	-77.5215	-81.6318	-78.6091	-77.9280
Pred. R^2	0.9938	0.9935	0.9931	0.9938	0.9935	0.9931	0.9938	0.9935	0.9932
Male Series									
$\log_{10}(\hat{a}_3)$	-0.6526*	-1.0873*	-1.2332*	-0.9309*	-1.3656*	-1.5116*	-1.9224*	-2.3578*	-2.5041*
\hat{b}_3	1.8119*	1.1509*	0.9289*	1.8126*	1.1516*	0.9294*	1.8251*	1.1633*	0.9406*
\hat{c}_3	-0.1406	-0.4365*	-0.5361*	-0.1403	-0.4362*	-0.5358*	-0.1348	-0.4309*	-0.5308*
\hat{d}_3	-0.0395*	-0.0797*	-0.0933*	-0.0395*	-0.0797*	-0.0933*	-0.0388*	-0.0790*	-0.0926*
AICc	-60.9665	-50.1556	-42.3794	-60.9753	-50.1627	-42.3803	-61.1423	-50.2830	-42.4619
Pred. R^2	0.9905	0.9877	0.9853	0.9905	0.9877	0.9853	0.9905	0.9877	0.9853

*indicates significant regression coefficient at 95% confidence level without Bonferroni correction.

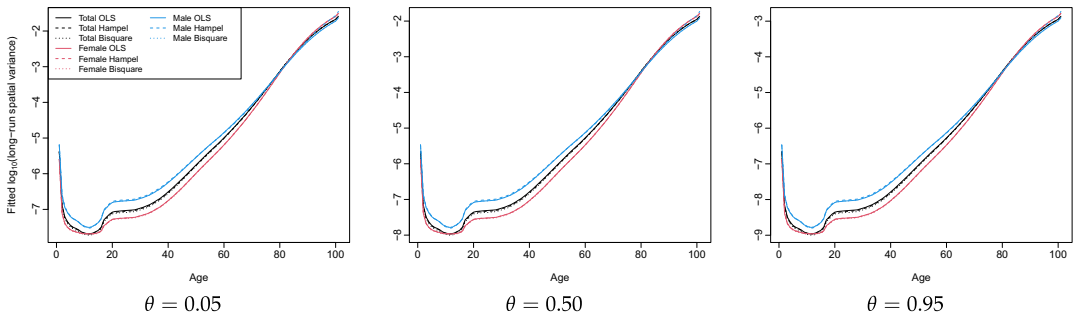


FIGURE 9 Fitted cubic long-run spatial-temporal TL regressions for $\theta=0.05, 0.50, 0.95$ for total, female and male mortality series in Japan. [Colour figure can be viewed at [wileyonlinelibrary.com](https://onlinelibrary.wiley.com/doi/10.1111/rssa.12899)]


5 | CONCLUSION

We propose several extensions of the log-linear TL model of human mortality. These proposed methods incorporate long-term variation and spatial correlation of non-negative measurements for multiple populations and minimize the impact of unusual observations on the estimated parameter. Applied to age-specific mortality rates of 47 prefectures in Japan from 1975 to 2018, the proposed new methods provide slope estimates less influenced by extreme events than the conventional TL. The proposed long-run spatial covariance can be applied to a wide range of research topics beyond animal and plant populations, for example analysing spatial and temporal distributions of firms in various industry sectors.

The principal new empirical results that emerge from our analysis of the Japanese prefectural age-specific mortality rates are:

1. Male and female humans in Japan have different temporal and spatial distributions of mortality rates. The cubic TL specification is better at capturing patterns of human mortality than the conventional linear TL model.
2. Natural disasters causing significant fatalities, such as the great Hanshin earthquake in 1995 and the massive tsunami in 2011, inflate spatial variances of subnational mortality. The robust estimation method with bisquare weights can reduce the influences of natural disasters on spatial TL estimates.
3. Temporal variances of mortality are different for 47 prefectures, indicating diverse changes in mortality in Japan. One reason for the uneven temporal variances is natural disasters increasing mortality in certain years for a group of prefectures. Another important factor for heterogeneity in temporal variances of mortality is the unbalanced economic development in Japan. Populations living in prefectures with high GDP tend to have TL coefficient estimates different from those with low GDP after removing outliers caused by earthquakes and tsunami.
4. As one referee pointed out, distances between prefectures as a measurement of spatial correlation between areas may not perfectly reveal asymmetric relationships between locations. For example, municipalities with better economic conditions and higher human capital stock in Japan are more likely to experience positive domestic population inflow (Higa et al., 2019). In contrast, non-metropolitan areas are experiencing depopulation and rapid ageing of residents. The impacts of domestic migration of the working-age population on the mortality patterns of large metropolitan cities, such as Tokyo, would be

better captured by human capital and wealth flows from other prefectures than simply using geographical distances. In future research, we would explore how domestic migration data can improve analysing the spatial correlation of human mortality in Japan.

Apart from the Japanese subnational mortality, the methods can also be applied to other subnational mortality, including Australia, Canada, France and the United States. Apart from human mortality rates, the proposed method can also be applied to animal and plant populations, for example voles in Hokkaido. To facilitate reproducibility, the  code for implementing the proposed methods and the Shiny app for visualizing the Japanese subnational mortality patterns are available at https://github.com/hanshang/Taylor_law.

The current paper proposes a cubic TL specification that uses scalar coefficients $\{a_3, b_3, c_3, d_3\}$ in Equation (5) to model human mortality rates for all ages between 0 and 100. Compared to the conventional linear TL model, the cubic TL model fits mortality rates better in the age intervals [1,10] and [90,100]. It is possible to integrate the age-varying relationship between mean and variance of human mortality into the TL coefficients. We shall examine a varying-coefficient TL model whose coefficients are smooth functions of ages in future research.

Our analysis extends prior research by taking account of correlations in mortality rates of each age group over time (autocorrelations) and across space (synchrony). The proposed methods can be further extended to incorporate correlations in mortality rates between different ages over time or across space, which topic is left for future research.

ORCID

Yang Yang  <https://orcid.org/0000-0002-8323-1490>

Han Lin Shang  <https://orcid.org/0000-0003-1769-6430>

Joel E. Cohen  <https://orcid.org/0000-0002-9746-6725>

REFERENCES

- Aida, J., Hikichi, H., Matsuyama, Y., Sato, Y., Tsuboya, T., Tabuchi, T. et al. (2017) Risk of mortality during and after the 2011 Great East Japan Earthquake and Tsunami among older coastal residents. *Scientific Reports*, 7(1), 1–11.
- Anderson, R., Gordon, D., Crawley, M. & Hassell, M. (1982) Variability in the abundance of animal and plant species. *Nature*, 296(5854), 245–248.
- Anderson, R.T., Sorlie, P., Backlund, E., Johnson, N. & Kaplan, G.A. (1997) Mortality effects of community socioeconomic status. *Epidemiology*, 8(1), 42–47.
- Andrews, D.W.K. (1991) Heteroskedasticity and autocorrelation consistent covariance matrix estimation. *Econometrica*, 59(3), 817–858.
- Bartlett, M.S. (1946) On the theoretical specification and sampling properties of autocorrelated time-series. *Supplement to the Journal of the Royal Statistical Society*, 8(1), 27–41.
- Ben-Shlomo, Y., White, I.R. & Marmot, M. (1996) Does the variation in the socioeconomic characteristics of an area affect mortality? *BMJ*, 312(7037), 1013–1014.
- Benassi, F. & Naccarato, A. (2019) Modelling the spatial variation of human population density using Taylor's power law, Italy, 1971–2011. *Regional Studies*, 53(2), 206–216.
- Bienvenido-Huertas, D., Pulido-Arcas, J.A., Rubio-Bellido, C. & Pérez-Fargallo, A. (2020) Influence of future climate changes scenarios on the feasibility of the adaptive comfort model in Japan. *Sustainable Cities and Society*, 61, 102303.
- Bohk, C., Rau, R. & Cohen, J.E. (2015) Taylor's power law in human mortality. *Demographic Research*, 33, 589–610.

- Carracedo, P., Debón, A., Iftimi, A. & Montes, F. (2018) Detecting spatio-temporal mortality clusters of European countries by sex and age. *International Journal for Equity in Health*, 17(1), 1–9.
- Cohen, J.E. & Saitoh, T. (2016) Population dynamics, synchrony, and environmental quality of Hokkaido voles lead to temporal and spatial Taylor's laws. *Ecology*, 97(12), 3402–3413.
- Cohen, J.E., Xu, M. & Brunborg, H. (2013) Taylor's law applies to spatial variation in a human population. *Genus*, 69(1), 25–60.
- Cohen, J.E., Poulin, R. & Lagrue, C. (2016) Linking parasite populations in hosts to parasite populations in space through Taylor's law and the negative binomial distribution. *Proceedings of the National Academy of Sciences of the United States of America*, 114(1), E47–E56.
- Cohen, J.E., Brunborg, H. & Xu, M. (2018) Can Taylor's law of fluctuation scaling and its relatives help demographers select more plausible multi-regional population forecasts? *Vienna Yearbook of Population Research*, 16, 15–23.
- Cohen, J.E., Bohk-Ewald, C. & Rau, R. (2018a) Gompertz, Makeham, and Siler models explain Taylor's law in human mortality data. *Demographic Research*, 38, 773–842.
- Cohen, J.E., Bohk-Ewald, C. & Rau, R. (2018b) Why does Taylor's law in human mortality data have slope less than 2, contrary to the Gompertz model? *Demographic Research response letter*. Available from: https://www.demographic-research.org/volumes/vol38/29/letter_67.pdf
- Coulmas, F. (2007) *Population decline and ageing in Japan – the social consequences*. New York: Routledge.
- Dey, S. & Joshi, A. (2006) Stability via asynchrony in *Drosophila* metapopulations with low migration rates. *Science*, 312(5772), 434–436.
- Ding, C. & He, X. (2004) K-means clustering via principal component analysis. In: *Proceedings of the twenty-first international conference on Machine learning*. Banff, Canada, p. 29.
- Donoho, D.L. & Huber, P.J. (1983) The notion of breakdown point. In: Bickel, P.J., Doksum, K. & Hodges, J.J.L. (Eds.) *A Festschrift for Lehmann, E. L.* Belmont, CA: Wadsworth, pp. 157–184.
- Eisler, Z., Bartos, I. & Kertész, J. (2008) Fluctuation scaling in complex systems: Taylor's law and beyond. *Advances in Physics*, 57(1), 89–142.
- Faraway, J.J. (2014), *Linear models with R*, 2nd edition, Boca Raton, FL: CRC Press.
- Fukuda, Y., Nakamura, K. & Takano, T. (2005) Cause-specific mortality differences across socioeconomic position of municipalities in Japan, 1973–1977 and 1993–1998: Increased importance of injury and suicide in inequality for ages under 75. *International Journal of Epidemiology*, 34(1), 100–109.
- Gao, Y., Shang, H.L. & Yang, Y. (2019) High-dimensional functional time series forecasting: an application to age-specific mortality rates. *Journal of Multivariate Analysis*, 170, 232–243.
- Geary, R.C. (1954) The contiguity ratio and statistical mapping. *The Incorporated Statistician*, 5(3), 115–146.
- Gilpin, M.E. & Hanski, I. (Eds.) (1991) *Metapopulation dynamics: empirical and theoretical investigations*. New York: Academic Press.
- Hampel, F.R. (1974) The influence curve and its role in robust estimation. *Journal of the American Statistical Association*, 69(346), 383–393.
- Hanski, I. (1999) *Metapopulation ecology*. Oxford: Oxford University Press.
- Hao, K., Yasuda, S., Takii, T., Ito, Y., Takahashi, J., Ito, K. et al. (2012) Urbanization, life style changes and the incidence/in-hospital mortality of acute myocardial infarction in Japan: report from the MIYAGI-AMI registry study. *Circulation Journal*, 76(5), 1136–1144.
- Higa, K., Nonaka, R., Tsurumi, T. & Managi, S. (2019) Migration and human capital: evidence from Japan. *Journal of the Japanese and International Economies*, 54, 101051.
- Hijmans, R.J. (2019) geosphere: Spherical Trigonometry. R package version 1.5-10. Available from: <https://CRAN.R-project.org/package=geosphere>
- Hoaglin, D., Mosteller, F. & Tukey, J. (1983) *Understanding robust and exploratory data analysis*. New York: John Wiley and Sons, Inc.
- Hörmann, S., Kidziński, L. & Hallin, M. (2015) Dynamic functional principal components. *Journal of the Royal Statistical Society: Series B*, 77(2), 319–348.
- Jannetta, A.B. & Preston, S.H. (1991) Two centuries of mortality change in central Japan: the evidence from a temple death register. *Population Studies*, 45(3), 417–436.
- Japanese Mortality Database. (2021) National Institute of Population and Social Security Research. Available from: <http://www.ipss.go.jp/p-toukei/JMD/index-en.html> (data downloaded on August 30, 2020).

- Kim, G.M. (2000) Multivariate outliers and decompositions of Mahalanobis distance. *Communications in Statistics – Theory and Methods*, 29(7), 1511–1526.
- Kokoszka, P., Rice, G. & Shang, H.L. (2017) Inference for the autocovariance of a functional time series under conditional heteroscedasticity. *Journal of Multivariate Analysis*, 162, 32–50.
- Li, Z.-C., Morikawa, Y., Nakagawa, H., Tabata, M., Nishijo, M., Semma, M. et al. (1994) Comparative study on mortality patterns in Japan and China. *Nippon Eiseigaku Zasshi (Japanese Journal of Hygiene)*, 49(5), 902–913.
- Li, D., Robinson, P.M. & Shang, H.L. (2020) Long-range dependent curve time series. *Journal of the American Statistical Association: Theory and Methods*, 115(530), 957–971.
- Martínez-Hernández, I., Gonzalo, J. & González-Farías, G. (2020) Nonparametric estimation of functional dynamic factor model, Working paper, King Abdullah University of Science and Technology. Available from: <https://arxiv.org/abs/2011.01831>
- Moran, P.A. (1950) Notes on continuous stochastic phenomena. *Biometrika*, 37(1/2), 17–23.
- Naccarato, A. & Benassi, F. (2018) On the relationship between mean and variance of world's human population density: a study using Taylor's power law. *Letters in Spatial and Resource Sciences*, 11(3), 307–314.
- Nakahara, S. & Ichikawa, M. (2013) Mortality in the 2011 Tsunami in Japan. *Journal of Epidemiology*, 23(1), 70–73.
- OECD. (2019) Pensions at a Glance 2013: OECD and G20 indicators, Technical report, OECD Publishing. Available from: <https://www.oecd.org/pensions/oecd-pensions-at-a-glance-19991363.htm>
- OECD. (2020) Regional economy data, Technical report, OECD Publishing. Available from: https://stats.oecd.org/OECDStat_Metadata/ShowMetadata.ashx?Dataset=REGION_ECONOM&ShowOnWeb=true&Lang=en (data downloaded on September 20, 2020).
- Parzen, E. (1957) On consistent estimates of the spectrum of stationary time series. *Annals of Mathematical Statistics*, 28(2), 329–348.
- Perry, J.N. & Taylor, L.R. (1985) Adès: new ecological families of species-specific frequency distributions that describe repeated spatial samples with an intrinsic power-law variance-mean property. *Journal of Animal Ecology*, 54(3), 931–953.
- Poulain, M. (2011) Exceptional longevity in Okinawa: a plea for in-depth validation. *Demographic Research* 25, 245–284.
- Reuman, D.C., Zhao, L., Sheppard, L.W., Reid, P.C. & Cohen, J.E. (2017) Synchrony affects Taylor's law in theory and data. *Proceedings of the National Academy of Sciences of the United States of America*, 114(26), 6788–6793.
- Rice, G. & Shang, H.L. (2017) A plug-in bandwidth selection procedure for long-run covariance estimation with stationary functional time series. *Journal of Time Series Analysis*, 38(4), 591–609.
- Rogers, A. (1995) *Multiregional demography: principles, methods and extensions*. New York: John Wiley.
- Rogers, A. (2008) Demographic modeling of the geography of migration and population: a multiregional perspective. *Geographical Analysis* 40(3), 276–296.
- Shang, H.L. (2019) Dynamic principal component regression: application to age-specific mortality forecasting. *ASTIN Bulletin: The Journal of the IAA*, 49(3), 619–645.
- Statistics Bureau Ministry of Internal Affairs and Communications. (2020) Statistical Handbook of Japan 2020. Available from: <https://www.stat.go.jp/english/data/handbook/index.html>
- Suzuki, M., Willcox, B. & Willcox, C. (2004) Successful aging: secrets of Okinawan longevity. *Geriatrics & Gerontology International*, 4(s1), S180–S181.
- Takata, H., Ishii, T., Suzuki, M., Sekiguchi, S. & Iri, H. (1987) Influence of major histocompatibility complex region genes on human longevity among Okinawan-Japanese centenarians and nonagenarians. *Lancet*, 330(8563), 824–826.
- Tamakoshi, T. & Hamori, S. (2015) Health-care expenditure, GDP and share of the elderly in Japan: a panel cointegration analysis. *Applied Economics Letters*, 22(9), 725–729.
- Tanida, N. (1996) What happened to elderly people in the great Hanshin earthquake. *BMJ*, 313(7065), 1133–1135.
- Tapia Granados, J.A. (2008) Macroeconomic fluctuations and mortality in postwar Japan. *Demography*, 45, 323–343.
- Tarsi, K. & Tuff, T. (2012) Introduction to population demographics. *Nature Education Knowledge*, 3(11), Article number: 3.
- Taylor, L.R. (1961) Aggregation, variance and the mean. *Nature*, 189(4766), 732–735.

- Taylor, L.R. (1984) Assessing and interpreting the spatial distributions of insect populations. *Annual Review of Entomology*, 29, 321–357.
- Taylor, R.A. (2019) *Taylor's power law: order and pattern in nature*. New York: Academic Press.
- Taylor, L.R. & Woiwod, I.P. (1980) Temporal stability as a density-dependent species characteristic. *Journal of Animal Ecology*, 49(1), 209–224.
- Taylor, L.R. & Woiwod, I.P. (1982) Comparative synoptic dynamics. I. Relationships between inter- and intra-specific spatial and temporal variance/mean population parameters. *Journal of Animal Ecology*, 51(3), 879–906.
- Taylor, L.R., Woiwod, I.P. & Perry, J.N. (1978) The density-dependence of spatial behaviour and the rarity of randomness. *Journal of Animal Ecology*, 47(2), 383–406.
- Taylor, L.R., Woiwod, I.P. & Perry, J.N. (1980) Variance and the large scale spatial stability of aphids, moths and birds. *Journal of Animal Ecology*, 49(3), 831–854.
- Turi, K.N. & Grigsby-Toussaint, D.S. (2017) Spatial spillover and the socio-ecological determinants of diabetes-related mortality across US counties. *Applied Geography* 85, 62–72.
- Willcox, D.C., Willcox, B.J., Shimajiri, S., Kurechi, S. & Suzuki, M. (2007) Aging gracefully: a retrospective analysis of functional status in Okinawan centenarians. *American Journal of Geriatric Psychiatry*, 15(3), 252–256.
- Woods, R. (2003) Urban-rural mortality differentials: an unresolved debate. *Population and Development Review* 29(1), 29–46.
- World Cities Database. (2021) Japan Cities Database. Available from: <https://simplemaps.com/data/jp-cities> (data downloaded on August 30, 2020).
- Xu, M. & Cohen, J.E. (2019) Analyzing and interpreting spatial and temporal variability of the United States county population distributions using Taylor's law. *PLoS ONE*, 14(12), e0226096.
- Xu, M., Brunborg, H. & Cohen, J.E. (2017) Evaluating multi-regional population projections with Taylor's law of mean-variance scaling and its generalization. *Journal of Population Research*, 34(1), 79–99.
- Yang, T.-C., Noah, A.J. & Shoff, C. (2015) Exploring geographic variation in US mortality rates using a spatial Durbin approach. *Population, Space and Place*, 21(1), 18–37.

SUPPORTING INFORMATION

Additional supporting information may be found in the online version of the article at the publisher's website.

How to cite this article: Yang, Y., Shang, H.L. & Cohen, J.E. (2022) Temporal and spatial Taylor's law: Application to Japanese subnational mortality rates. *Journal of the Royal Statistical Society: Series A (Statistics in Society)*, 185(4), 1979–2006. Available from: <https://doi.org/10.1111/rssa.12859>